LBNL Sustainable Systems SFA: Predicting Contaminant Mobility Challenge
Predicting Plume-Scale U and ^{90}Sr Mobility at the Savannah River Site

Nicolas Spycher[1], John N. Christensen[1], Sudipta Rakshit[1], Jiamin Wan[1], Susan S. Hubbard[1], Arthur Wiedmer[2], and Miles Denham[3]

[1]Lawrence Berkeley National Laboratory; [2]University of California, Berkeley; [3]Savannah River National Laboratory

ABSTRACT

Low-level radioactive, acid waste solutions were disposed into seepage basins at the F-Area of the Savannah River Site from 1955 to 1989. As a result, an acidic plume has developed in groundwater beneath the basins. The plume contains many contaminants, including various U isotopes, ^{90}Sr, ^{129}I, ^{99}Tc, tritium, and nitrate, with pH values as low as 3.2. After a decade of active remediation, natural attenuation is now being considered as a long-term remediation alternative at this site.

CHALLENGES

- Accurate characterization and prediction of plume distribution at the plume scale
- Understanding the relationship between key geochemical processes (grain scale) and plume migration (large scale)
- Determine the level of characterization and model complexity sufficient to predict system behavior over long time frames
- Develop computationally-efficient, mechanistic (as opposed to empirical) reactive transport models

HYPOTHESES

- **HYPOTHESIS 1:** Specific types of sediments display similar and relatively homogeneous characteristics affecting U and Sr sorption/ precipitation behavior in the subsurface
- **HYPOTHESIS 2:** Reactive transport properties and mechanisms can be assigned spatially using a concept of *reactive facies* to provide model input with sufficient complexity over field-relevant scales
- **HYPOTHESIS 3:** An optimal level of model complexity for prediction of contaminant mobility at the plume scale can be identified, beyond which model accuracy does not increase significantly

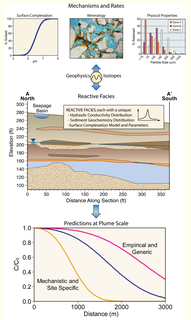

Figure 1. Conceptual illustration of approach followed to evaluate contaminant mobility at the plume scale.

Objectives

- Develop efficient predictive capabilities to assess contaminant behavior at the plume scale
- Evaluate natural attenuation over stewardship timeframes

Approach

- Identify specific *reactive facies*, representing unique reactive transport properties for specific types of sediments
- Use a variety of laboratory and field-scale geochemical, geophysical, and isotopic methods
- Focus on U and ^{90}Sr
  - -Strong partitioning into sediments upon pH rise
  - -Long-term risk drivers
- Three-prong research activities (Fig. 1):
  - -Investigate the hierarchy of mechanisms controlling natural attenuation
  - -Parameterize mechanistic reactive transport models
  - -Assess the level of complexity sufficient and necessary for successful long-term predictions

These efforts will be used to parameterize reactive transport models of the site at various scales and with various levels of complexity. This will ultimately include a plume-scale model to assess the natural attenuation capacity of the F Area.

BACKGROUND

F-AREA

- Processing facility that extracted Pu from irradiated depleted uranium targets, and discharged low-level radioactive process solutions into seepage basins (Figs. 2 and 3)
- Discharged solutions typically of low pH (~2), high nitrate, tritium, ^{90}Sr, ^{137}Cs, U isotopes, Pu isotopes, ^{99}Tc, and ^{129}I concentrations, with small amounts of other radionuclides
- Large acidic groundwater plume (Fig. 4), primarily ^{90}Sr, U isotopes, ^{129}I, ^{99}Tc, nitrate, tritium, pH ranging ~3.2 to 4.5
- About 100 monitoring wells, some with 25 years of monitoring records
- Basins capped in 1991 after 40 years of operation (Fig. 3)
- Pump-and-treat remediation since 1997 then replaced in 2004 by a funnel-and-gate system (Fig. 4)
- Monitored natural attenuation is considered for the core of the plume

Figure 2. Site location map.

Figure 3. F-Area impoundments before and after capping.

HYDROGEOLOGY

- Altantic Costal Plain unconsolidated and semi-consolidated clayey sands (primarily quartz, kaolinite, Fe oxyhydroxides) (Fig. 5)
- Multi-aquifer system with bulk of contamination in water-table aquifer underlain by locally confining clay layer (Fig. 6, Table 1)
- Dilute Ca/Na bicarbonate waters (TDS < 200 mg/L) with low pH typically ~5.5 at shallow depth and increasing in deeper units (Fig. 7)
- Typically high hydraulic conductivity and seepage velocity (Table 1)

Figure 4. F-Area contaminant plume and current remediation system.

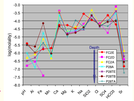

Figure 7. Typical background water quality at the F-area.

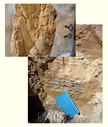

Figure 5. Upper Aquifer sand/clayey sand units.

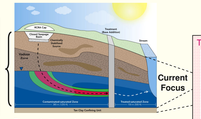

Figure 6. Illustration of the Upper Aquifer Zone and contaminant migration.

Table 1. Hydrostratigraphic units and typical flow properties

Hydrostratigraphic Unit		Hydraulic Conductivity (m/day)	Effective Porosity	Groundwater Velocity (m/year)
UTR	Upper, Upper Three Runs Aquifer Zone	8	0.20	121
UAZ				
TCCZ	Tan Clay Confining Zone	9×10^{-6}	0.15	0.7
UTR	Lower, Upper Three Runs Aquifer ZONE	0.6	0.20	6.5
LAZ				
GCU	Gordon Confining Unit	3×10^{-6}	0.12	0.08
GAU	Gordon Aquifer Unit	12	0.25	77

ONGOING INVESTIGATIONS AND RESULTS

NUMERICAL MODELING. Geochemical and reactive transport simulations are being used to help evaluate the results of laboratory investigations, as well as to assess factors affecting natural attenuation. The effect of elevated Al concentrations in the acidic plume (Fig. 8) has been investigated. Al appears to significantly delay pH recovery when the plume water mixes and reacts with clean background water (Fig. 9).

Path Forward. Reactive transport models with increasing levels of complexity are being built. These will incorporate U and ^{90}Sr surface complexation models based on field data and definitions of reactive facies as derived from laboratory and geophysical investigations.

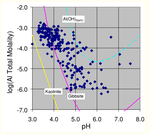

Figure 8. Al concentrations versus pH along the core of the F-Area plume. Lines show computed equilibrium boundaries for potential controlling phases (these boundaries may shift up or down depending on thermodynamic data sources).

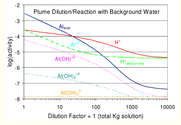

Figure 9. Simulated mixing between acid plume water at pH 3.2 and background water at pH 5.4. The precipitation of Al hydroxides (here taken as gibbsite) and/or kaolinite-type clay minerals delays pH recovery because it involves hydrolysis (e.g., $Al^{+3} + 3H_2O = Al(OH)_{3(s)} + 3H^+$). The green curve shows much faster pH recovery by dilution alone (i.e. without precipitation of Al hydroxides and/or clays).

ONGOING INVESTIGATIONS AND RESULTS

LABORATORY INVESTIGATIONS. Sediments and porewater from new boreholes (Fig. 10) are being characterized to develop site specific surface complexation models, evaluate the concept of reactive facies, and help understand natural attenuation mechanisms at the site.

Methods. Porewater was extracted from sediment cores (collected at new boreholes FAW-1, 2, 4, and 5) by centrifugation at 4000 rpm for 15 minutes using centrifuge tubes with 0.2 µm membrane filter paper. The porewater was analyzed for ^{238}U using a Kinetic Phosphorescence Analyzer. Bicarbonate extraction[1] was used to obtain surface-bound ^{238}U. Field partition coefficients (K_d=1000*C_s/C) were calculated taking sorbed ^{238}U as the bicarbonate-extractable ^{238}U (C_s, in $\mu g_{sorbed}/g_{soil}$) and total dissolved ^{238}U in pore water (C, in µg /L).

Results. The concentration of ^{238}U in sediment porewater is highest at FAW-2 (Fig. 11). At FAW-1, no ^{238}U was detected. Many porewater samples at FAW-2, 3, and 4 have ^{238}U concentrations above the U.S. EPA Maximum Contaminant Level (MCL) of 30 µg/L. There appears to be no correlation between porewater ^{238}U concentrations and depth (Fig. 11). However, bicarbonate-extractable ^{238}U concentrations appear to increase with depth, with highest concentrations reported at FAW-2 (Fig. 12). Porewater pH values range from 4 to 7.5 (Fig. 13). Calculated field K_d values generally increase with pH (Fig. 14). No clear correlation is found between K_d and depth (Fig. 15). Potential correlations between K_d values, sediment type, grain size, and mineralogy are being investigated.

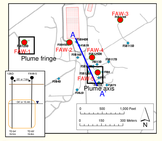

Figure 10. Location of new boreholes (red circles) drilled in Summer 2008. FAW-1, 3, 4, 5 are vertical, FAW-2 is inclined under the basin. Black rectangles delineate areas of geophysical investigations, with inset showing tomographic cross-sections near FAW-5. The blue line shows the location of the geologic cross-section in Fig. 16.

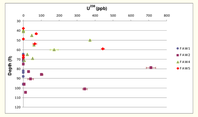

Figure 11. U^{238} concentration in sediment porewaters versus depth at various locations.

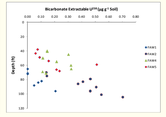

Figure 12. Bicarbonate-extractable U^{238} concentrations versus depth at various locations.

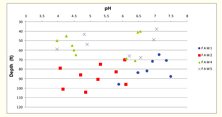

Figure 13. Sediment porewater pH versus depth at various locations.

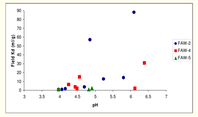

Figure 14. Calculated field K_d values as a function of sediment porewater pH at various locations.

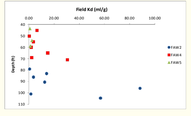

Figure 15. Calculated field K_d values as a function of depth at various locations.

GEOPHYSICAL CHARACTERIZATION. Geophysical datasets have been collected between new and existing boreholes (Fig. 10) to test the geophysical signatures of various sediment types.

First Field Campaign. Field radar and seismic tomographic data were collected within two different local-scale test sites (Fig. 10) in January 2009: along the plume axis at FAW-5 (Fig. 16) and on the plume fringe at FAW-1 (Fig. 17).

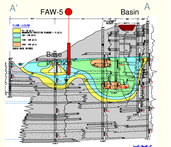

Figure 16. Geologic cross-section A-A' (see Fig. 10 for location) along the plume axis, with new borehole FAW-5 shown.

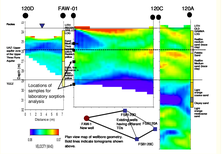

Figure 17. Radar velocity profile near new borehole FAW-1 (see Fig. 10 for location).

ONGOING INVESTIGATIONS AND RESULTS

IDENTIFICATION OF REACTIVE FACIES. Geophysical data are being evaluated together with existing hydrogeologic data, new laboratory measurements, and isotopic data to define various reactive facies and extrapolate them at the plume scale.

Data Quality and Next Steps. Inversion and early comparison with existing hydrogeological data suggest that:

- ➢The tomographic data quality is good and geophysical attribute variations are evident within and between facies
- ➢A second field geophysical campaign is planned for Summer 2009
- ➢The geophysical attributes will be compared with wellbore and laboratory-derived hydrogeochemical information in the iterative identification of reactive facies
- ➢Once identified, tomographic and surface-based geophysical data will be used to assign reactive facies spatially as needed to provide model input with sufficient complexity over field-relevant scales

Estimation of Spatially Distributed Reactive Facies. A Bayesian approach will be used in the estimation of reactive facies. This approach will jointly consider laboratory and wellbore hydrogeochemical information, with crosshole and surface geophysical data (Fig 18).

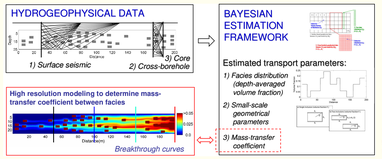

We will build upon a recently developed hydrofacies estimation framework that is currently being tested in the same hydrological section but in the Savannah P-Area (see Shafer et al. poster).

Figure 18. Illustration of joint geophysical and hydro-geochemical data inversion to spatially distribute reactive facies at the plume scale.

ISOTOPE STUDIES. Various isotopic analyses of groundwater and porewater samples are ongoing: $^{234}U/^{238}U$, $^{235}U/^{238}U$ and $^{236}U/^{238}U$ to map spatial variations and track the evolution of U sources, pathways, and their evolution; $\delta^{15}N$ and $\delta^{18}O$ to evaluate chemical changes in the plume; and $^{87}Sr/^{86}Sr$ to trace plume/sediment chemical interactions and track contaminant sources (direct analog to ^{90}Sr).

Figure 19. ^{238}U plume map for the Upper Aquifer Zone (3rdQ 2006; red numbers are activities in pCi/L).

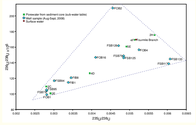

Figure 20. Relationship between various U isotope ratios indicating three potential end-member sources.

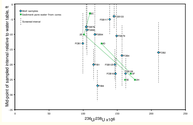

Figure 21. $^{236}U/^{238}U$ versus depth. Dashed lines show the screened interval in sampled wells. Green lines tie sediment samples from the same boreholes.

Results. Uranium isotopic compositions of porewater, groundwater, and surface water vary significantly amongst the sampled locations (Figs. 19 and 20) suggesting that U isotopes can be used to trace and fingerprint U contamination. Three distinct U contaminant end-members have been identified, all involving variably depleted U with distinct $^{236}U/^{238}U$ signatures (Fig. 20). In addition to horizontal U isotopic variations, results from precisely-located samples with depth (Fig. 21) indicates vertical variation, suggesting a U isotopic "stratigraphy", independent of concentration, that may be mapped to sediment facies.

REFERENCES

1. Kohler, M., G.P. Curtis, D.E. Meece, and J.A. Davis. 2004. Environ. Sci. Technol. 38:240-247.

Funding for this study was provided by the U.S. Department of Energy, BER Program Contract DE-AC020SCH11231 to the LBNL Sustainable Systems Scientific Focus Area